First-Principles Investigation of Black Phosphorus Synthesis

*Pola Shriber, Atanu Samanta, Gilbert Daniel Nessim, Ilya Grinberg**

Department of Chemistry, Bar-Ilan University, Ramat Gan, Israel 52900

Supplementary Section 1 (S1):

Computational Method for SIESTA code calculations:

It has been shown that the methods with linear scaling with respect to system size are a crucial tool for first-principles quantum mechanical studies of large systems containing many atoms [1,2]. Here, we have used the linear scaling *ab-initio* density functional method as implemented in the SIESTA4.0 package[2] for calculating total energy and structural optimization of the black phosphor (BP), red phosphorus (RP) and their combinations with iodine and Sn metal clusters. The basis set of the electronic wave function is represented by the double-ζ basis including polarization orbitals (DZP). For phosphorus atom, an extra polarization orbital is included in the basis set. We have used improved norm-conserving Troullier-Martins pseudo-potentials[3,4] with the parameters taken from the PseudoDojo[5,6]. The pseudo-potentials were generated by considering core-correction[8] and relativistic corrections using the ATOM-4.2.6 code[7] for all atom types. The exchange-correlation energy of the electron is represented using the Perdew–Burke-Ernzerhof (PBE) functional within the generalized gradient approximation (GGA)[9]. We have considered $3s^2 3p^3$, $4d^{10} 5s^2 5p^2$, and $5s^2 5p^5$ valence electrons configuration for P, Sn, and I atom, respectively and used the density mesh cutoff of 300 Ry and Γ *k*-point sampling in our studies. The van der waals (vdW) interaction among the species is included by using the parameterized Grimme's D2 correction[11] . To avoid artificial Coulumbic interaction between the periodic images, a vacuum of ~15 Å is used. The atomic positions were optimized using the conjugate gradient methoduntil the residual Hellmann-Feynman forces were all < 0.02 eV/Å and total energy tolerance was $<10^{-4}$.

Supplementary Section 2 (S2):

Results and Discussion:

The enthalpy of formation (ΔH) per atom for black phosphorous (BP) and red phosphorous (RP) is calculated using the following formula

$$\Delta H_X = \frac{E_X^{Total} - N * E_{P_4}}{N} \quad \ldots\ldots\ldots\ldots\ldots\ldots (1)$$

Where E_X^{Total} and E_{P_4} are the total energy of the system X (X=RP or BP) and the energy per atom of the P_4 molecule, respectively. *N* is total number of the P atoms required to form system X (RP or BP). The enthalpies of formation calculated using QE and SIESTA are shown in Figs. S4 (a) and (b). The difference in the enthalpy of formation between BP and RP is positive, indicating that RP is thermodynamically stable phase when the P_4 molecules starts assembling to form RP or BP. The calculated values of enthalpy formation for RP and BP using the plane wave basis set based QE and numerical atomic orbital basis set based SIESTA codes show a similar trend as a function of P_4 unit, however the calculated values using SIESTA code differ by 0.2 eV/atom from those obtained using the QE code. By contrast, the relative change between BP and RP is for the SIESTA calculations differs by less than 0.02 eV/atom from the values obtained by the QE code. This difference arises due to different basis sets used to calculated the total energy of the RP and BP clusters.

Next, we have placed I atoms close to the strained P_4 edge groups in BP/ RP and optimized the structures, obtaining the structure shown in Figs. S1 (a) and (b). The enthalpy of formation of the compounds per P atom is calculated using following formula

$$\Delta H_{X+I} = (E_{X+I}^{Total} + (10 - m) * E_{I_2}) - N * E_{P_4} - 10 * E_{I_2})/\mathrm{N} \ldots\ldots\ldots\ldots (2)$$

where E_{X+I}^{Total} and E_{I_2} are the total energy of the system X (X=RP or BP) and energy per atom of the I_2 molecule, respectively. *m* is the total number of I atoms attached to X (RP or BP). The calculated enthalpies of formation using QE and SIESTA are shown in Figs. S4 (c) and (d). The difference in the enthalpy of formation between RP and BP decreases significantly due to the replacement of the strained P-P bonds at the edges of BP by the formed P-I bonds. The P-I bond length is ~ 2.48- 2.52 Å and the energy per P-I bond is –0.62 eV or 14.01kcal/mol. Such a small P-I bond energy is beneficial for the easy breaking P-I bonds which allows the removal of I and the growth of BP or RP. It is well-known in heterogeneous catalysis that the free energy of adsorption on the catalysts should be close to zero to enable the optimal combination of sufficiently rapid adsorption on the catalyst from the reactants as well as the subsequent desorption from the catalyst to form the products. Therefore, the low bond energy of the P-I bond is favorable for the I to act as a catalyst, first saturating the edge P atoms and providing unstrained P-I bonds and then breaking these bonds when the BP grows and the P-I bonds are replaced by unstrained P-P bonds due to the incorporation of the additional P_4 molecules into the BP structure.

To understand the role played by Sn in the formation of BP and RP, we assume that Sn will be found in the form of cluster in the liquid form and the cluster will interact with phosphorous atoms. The studies of the stabilities and structures of β- and α-Sn nanoparticles by Sabet and Kaghazchi also indicates that β-Sn particle will be stable at high temperature[10]. We have

considered 48-atom cluster of β-Sn (tetragonal high temperature phase). The optimized structures of RP and BP on 48 atoms of β-Sn cluster are shown in Figs. S2(a) and (b). The distance between the Sn atoms and P atoms is >2.7 Å, indicating significant vdW interaction between the Sn and P clusters. We have found that the enthalpy of formation for RP is still lower than that of BP as shown in Fig. S5 (a). However, the difference between BP and RP decreases compared to the difference between the freestanding BP and RP clusters. This implies that Sn alone cannot provide the higher stability to the BP relative to RP in the initial stages of the BP and RP growth process.

To understand the effects of I and Sn on the stability of BP and RP, we have placed the RP and BP along with I atoms attached to the P atoms above the Sn cluster and optimized the structures using DFT-D2 calculations as implemented in the SIESTA code. The optimized structures are shown in Figs. S3 (a) and (b). The ΔH is calculated as

$$\Delta H_{X+I} = \left(\left(E^{Total}_{X+I+Sn} + (10-m) * E_{I_2}\right) - N * E_{P_4} - 10 * E_{I_2} - E_{Sn}\right)/N \ldots\ldots\ldots\ldots\ldots\ldots (3)$$

where E_{Sn} and E^{Total}_{X+I+Sn} are total energy of the 48 atoms Sn cluster and total energy of the combined system of Sn, I and X (X=RP or BP). The calculated ΔH becomes lower for BP compared to RP, indicating that BP is thermodynamically more stable compared to RP as shown in Fig. S5 (b). The simulation also shows that some of P-I bonds length increase to nearly 3.0 Å suggesting Sn interaction also helps in the breaking of P-I bonds. Such P-I bond breaking is necessary for the growth of BP clusters and also for the stacking of large BP sheets to assemble the BP solid upon the solidification of Sn. Therefore, we conclude that vdW interaction between Sn and P and I-P chemical bonding are essential for synthesis of BP and both Sn and I play important catalytic roles in BP synthesis.

Supplementary Figure S1:

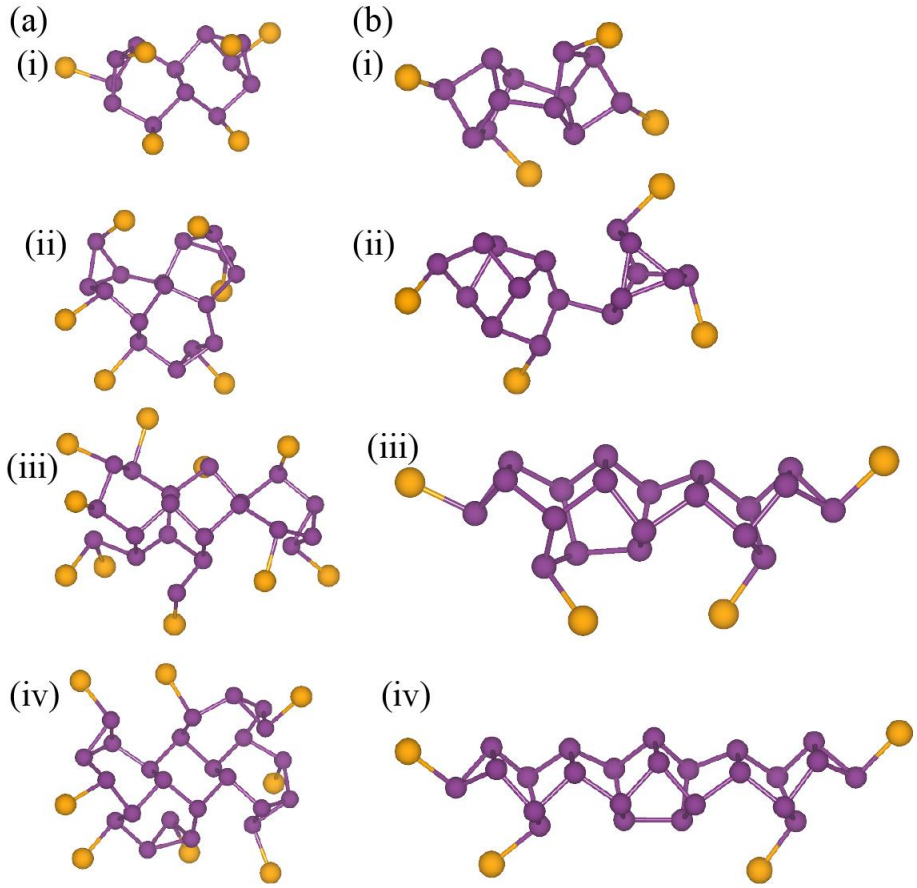

Figure S1 (a)-(i), (ii), (iii) and (iv) are optimized structures for 12, 16, 20 and 24 atoms black phosphorous (BP) and I atoms, respectively. (b)-(i), (ii), (iii) and (iv) are optimized structures for 12, 16, 20 and 24 atoms red phosphorous(BP) and I atoms, respectively. Blue and orange color balls represents P and I atom, respectively. P-I bonds length are in between 2.48 Å to 2.52 Å.

Supplementary Figure S2:

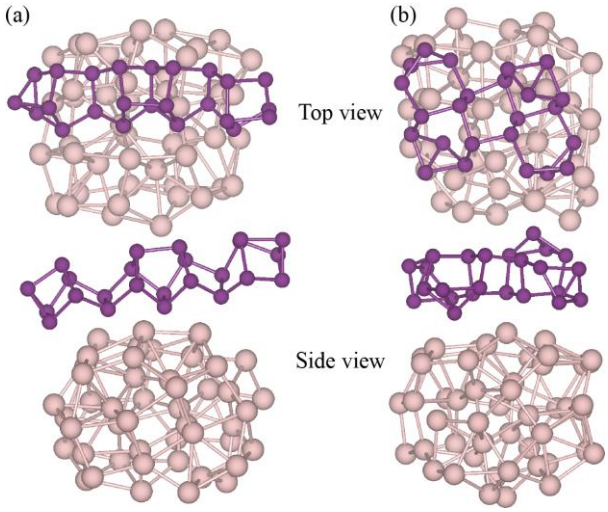

Figure S2 (a) and (b) are optimized structures of 24 atoms of RP and BP on 48 atoms Sn cluster. The distance between Sn cluster and P atoms of BP or RP is ~3.0Å. Blue and flamingo color balls represents P and Sn atom, respectively.

Supplementary Figure S3:

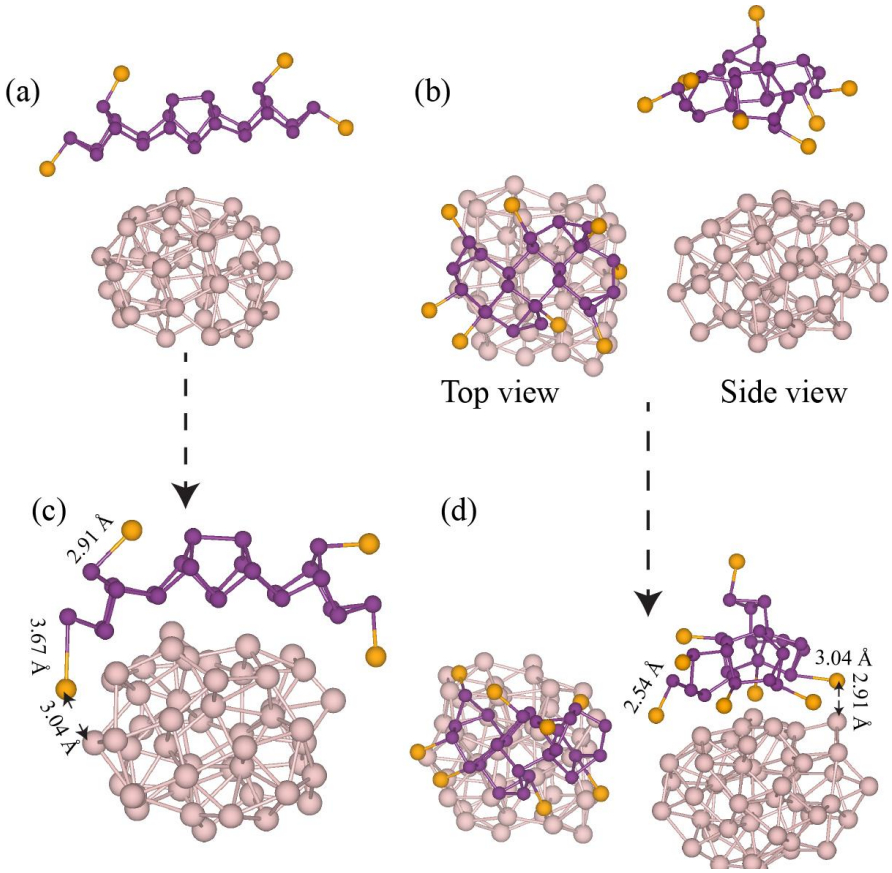

Figure S3 (a) and (b) are unoptimized structures of 24 atoms of RP+I and BP+I on 48 atoms Sn cluster. (c) and (d) are optimized structures of 24 atoms of RP+I and BP+I on 48 atoms Sn cluster. The distance between Sn cluster and P atoms of BP or RP is ~3.0Å. Blue, orange and flamingo color balls represent P, I and Sn atom, respectively.

Supplementary Figure S4:

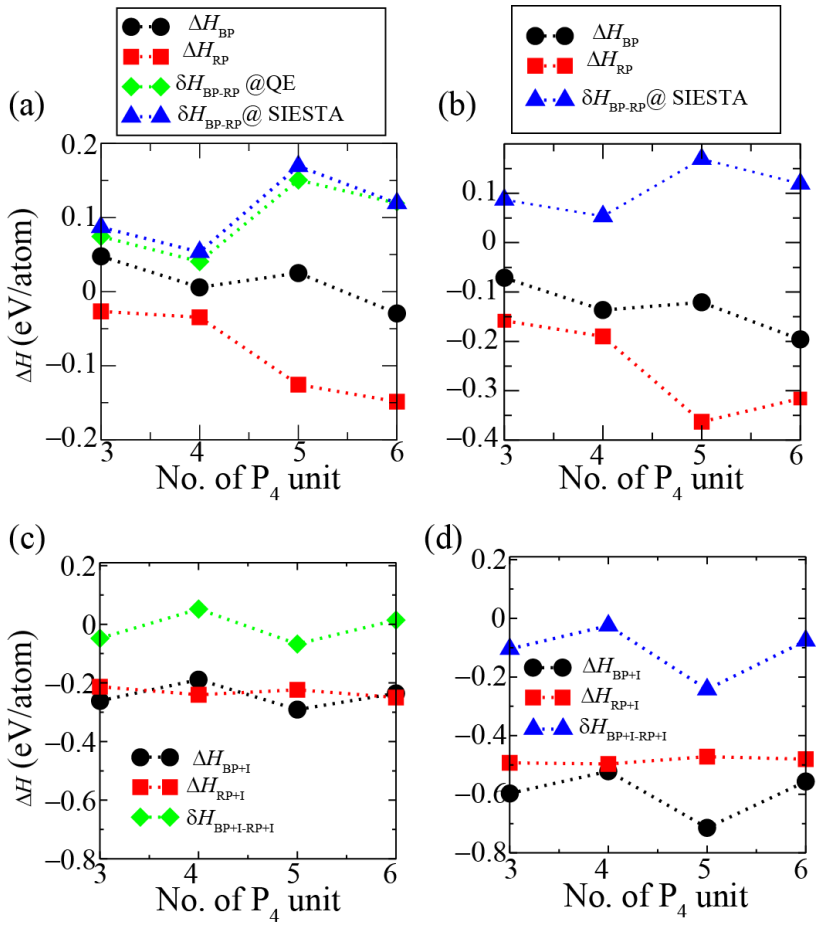

Figure S4: Enthalpy of formation energy per P atom (ΔH) as a function of number of P_4 unit for BP and RP. ΔH calculated using (a) QE package and (b) SIESTA package. ΔH is calculated using (c) QE and (d) SIESTA as a function of number of P_4 unit for BP and RP with I atoms. Diamond (calculated using QE) and triangle (calculated using SIESTA) filled with green and blue color symbols represent the difference of enthalpy of formation between RP and BP.

Supplementary Figure S5:

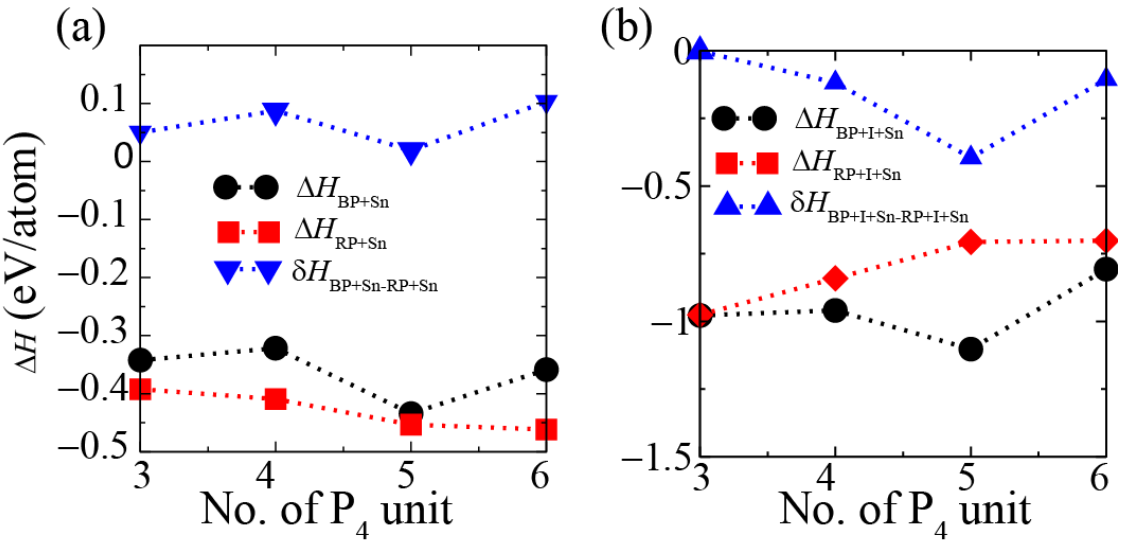

Figure S5: (a) ΔH as a function of number of P_4 unit for BP and RP with 48 atoms Sn cluster. (b) ΔH as a function of number of P_4 unit for BP and RP with I atoms and 48 atoms Sn cluster. Triangle filled with blue color represents the difference of enthalpy of formation between RP and BP. All data presented in this graph are calculated using SIESTA package.

Supplementary Figure S6:

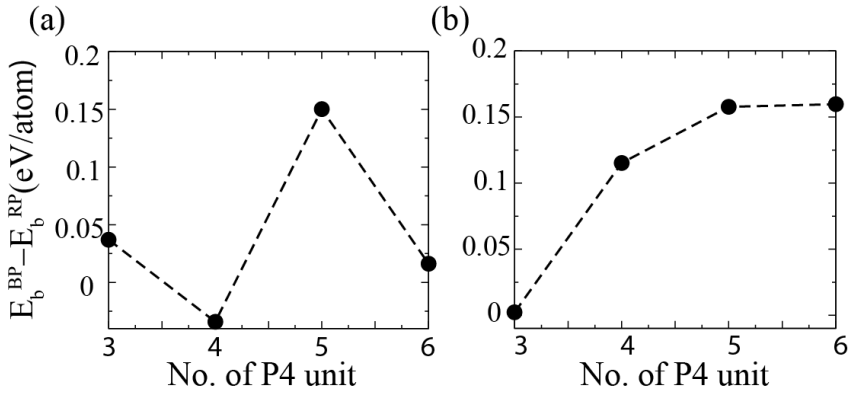

Figure S6: (a) binding energy difference between BP and RP on 48 atoms Sn cluster. (b)) binding energy difference between BP+I and RP+I on 48 atoms Sn cluster. The binding energy per atom of a structure X is calculated as $\boldsymbol{E_b^X = \frac{(E_X + E_{Sn}) - E_{X+Sn}}{N}}$, where E_X, E_{Sn} and E_{X+Sn} are the total energy of the structure X (where, X=RP, BP, BP+I and RP+I), 48 atoms Sn cluster, and X structure on top of 48 atoms Sn cluster. N is the total number of P atoms in structure X. The binding energy between BP and Sn cluster is higher than the RP and Sn, which favors the formation of BP. All data presented in this figure are obtained using the SIESTA package.

References:

(1) Stefan, G. Linear Scaling Electronic Structure Methods *Rev. Mod. Phys.* **1999**, *71*, 1085

(2) Soler, J.M.; Artacho, E.; Gale, J.D.; Garcia, A.; Junquera, J.; Ordejon, P.; Sanchez-Portal, D. The SIESTA Method for *ab-initio* O(N) Materials Simulation *Jour. Phys. Condens. Matter*. **2002,** *14*, 2745-2779

(3) Troullier, N.; Martins, J. L. Efficient Pseudo potentials for Plane-Wave Calculations. II. Operators for Fast Iterative Diagonalization *Phys. Rev. B*. **1991**, *43*, 8861

(4) Efficient Pseudopotentials for Plane-Wave Calculations, Troullier, N.; Martins, J. L. *Phys. Rev. B* **1991**, *43*, 1993

(5) van Setten, M. J.; Giantomassi, M.; Bousquet, E.; Verstraete, M.J.; Hamann, D. R.; Gonze, X.; Rignanese G.M. The PseudoDojo: Training and Grading a 85 Element Optimized Norm-Conserving Pseudopotential Table arXiv:1710.10138

(6) García, A.; Verstraete, M.; Pouillon, Y.; Junquera, J.; The PSML format and library for norm-conserving pseudopotential data curation and interoperability arXiv:1707.08938

(7) Froyen, S.; Troullier, N.J.; Martins, J.L.; Balbás, L.C.; Soler, J.M.; Garcia, A. ATOM-4.2.6.

(8) Louie, S.G.; Froyen, S.; Cohen, M.L.; Nonlinear Ionic Pseudopotentials in Spin-Density-Functional Calculations *Phys. Rev. B* **1982**, *26*, 1738

(9) Perdew, J.P.; Burke, K.; Ernzerhof, M.; Generalized Gradient Approximation Made Simple, *Phys. Rev. Lett.* **1996**, *77*, 3865; *Erratum Phys. Rev. Lett.* **1997**, *78*, 1396

(10) Sabet, S.; Kaghazchi, P. Communication: Nanosize-Induced Restructuring of Sn Nanoparticles, *J.Chem.Phys.* **2014**, *140*, 191102

(11) Grimme, S.; Semiempirical GGA-type density functional constructed with a long-range dispersion correction *J. Comput. Chem.* **2006**, *27*, 1787-1799